

# EXTENSION OF THE MIXED BOHM/GYRO-BOHM MODEL TO ELMY H-MODE AND FLAT OR REVERSED CENTRAL SHEAR DISCHARGES OF JET AND TORE SUPRA.

Erba M., Aniel T., Balet B.\*, Bécoulet A., Hoang G.T., Imbeaux F., Joffrin E., Litaudon X., Parail V.V.\*, Springmann E.\*, Taroni A.\*.

*Association Euratom-CEA, CEA-Cadarache 13108 Saint Paul-lez-Durance Cedex, FRANCE*

*\*JET Joint Undertaking, Abingdon, Oxfordshire, OX14 3EA.*

## 1. INTRODUCTION

A mixed Bohm/gyro-Bohm model for electron and ion heat transport [1] is a good candidate for describing several regimes of Tokamak operation. This model has already been successfully tested in L-mode, Hot-Ion H-mode and strongly transient regimes of JET, including cold pulses, L-H transitions, ELMs, sawteeth [1]. It is natural to extend it to other regimes as well as to test it on different machines, like the circular Tore Supra Tokamak (TS). In this work we first consider in detail the ELMy H-mode regime which is particularly promising for steady-state operation in a future reactor. We study discharges from  $\rho^*$ -scaling experiments performed in JET ELMy H-mode [2], as well as other ELMy H-mode discharges in JET, DIII-D, Alcator C-mod and Asdex Upgrade obtained from the ITER database [3]. For the L-mode regime we consider several representative discharges from the ITER database and then apply statistical analysis to the simulated dataset. Finally we present results of simulations of discharges in the Optimized Shear (OS) regime [4] from both JET and TS.

## 2. STEADY STATE ELMY H-MODE AND L-MODE REGIMES

We consider the expression of the ‘mixed’ model defined in [1] with the given values of the numerical coefficients. Important features of this model are the non-local dependence of the Bohm term on the edge temperature and the simple expression of the gyro-Bohm term, which is typically very small and peaked near the plasma centre in the L-mode regime in large machines. The gyro-Bohm term in L-mode can be important only in small machines, due to the increased value of  $\rho^*$ . The situation is different in H-mode, where the non-local dependence of the Bohm term on the edge temperature means that this term is reduced by the formation of an edge temperature pedestal so that the gyro-Bohm term becomes important in the inner region of the plasma column. Hence it will be useful in the following to consider alternative versions of the mixed model where the gyro-Bohm term has been modified.

In the case of the ‘mixed 98’ model we simply increase the numerical coefficient in front of the gyro-Bohm term by a factor 2, leaving everything else unchanged in the mixed model.

In the case on the ‘new mixed’ model we use a new expression of the gyro-Bohm term:

$$\chi_{GB} = \alpha_{GB} \frac{\sqrt{T_e} |\nabla p_e|}{n_e B_t^2} q^2 \left(\frac{r}{R}\right)^{1/2} \sqrt{\frac{A}{Z}} \quad (1)$$

with  $\alpha_{GB}=0.1$  (using keV, m, m<sup>2</sup>/s, T). We point out that in this case the gyro-Bohm term is no longer peaked near the centre, but it increases fast towards the edge and is comparable to the Bohm term in magnitude. Hence to maintain the same confinement we reduce the numerical coefficient of the Bohm term by a factor 2.

We have tested the above three models against a set of 8 ELMy H-mode discharges from the ITER database and 6 discharges from the JET database. The ITER database discharges include  $\rho^*$ -scaling experiments in DIII-D, density and temperature scaling experiments in DIII-D, and representative shots from Asdex Upgrade and Alcator C-Mod.

We carry out the simulations in quasi-stationary regimes using the code Astra [5], imposing the density profiles, power deposition profiles,  $Z_{eff}$  profiles taken from ITER database. We also impose the edge temperature so as to match the temperature value at  $x=\rho/\rho_{max}=0.8$ , where  $\rho$  is the toroidal flux coordinate. In this way we do not have to simulate in detail the transport barrier, which is in all our simulated discharges outside the  $x=0.8$  surface. Furthermore the experimental error on the temperature measured at  $x=0.8$  is much lower than at  $x=1$  (for this reason we shall apply the same procedure to L-mode shots).

Considering the JET  $\rho^*$ -scaling experiment, we find that the mixed 98 model works better than the other models in the 1 T case (Fig.(1)), while differences between models are smaller in the 2 T discharge (Fig.(2)).

These results prove that the gyro-Bohm term is necessary to describe electron confinement near the plasma centre, while the Bohm term dominates near the edge.

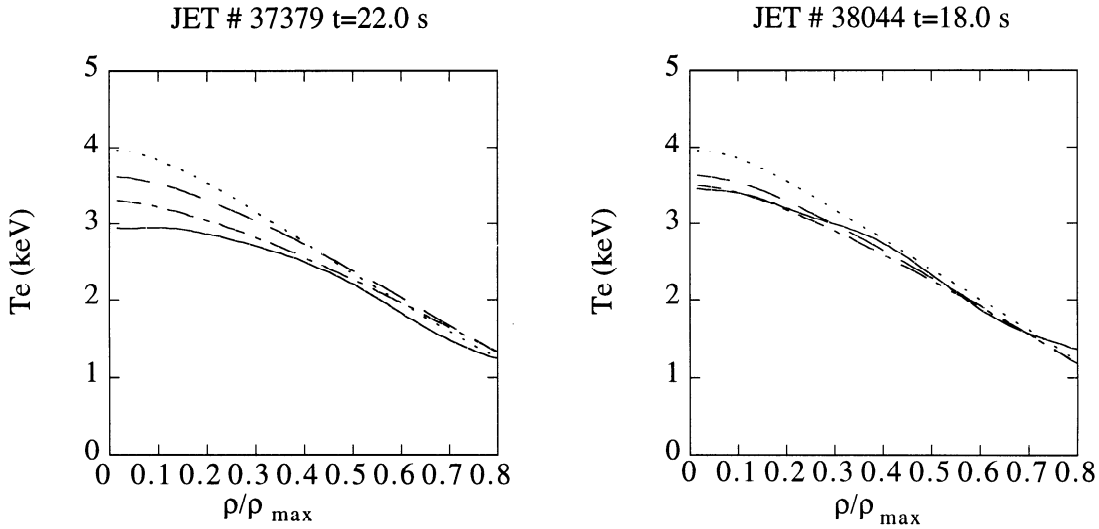
The above results are confirmed by computing the quantities:

$$m = \frac{1}{N} \sum_{0.3 < x < 0.8} \varepsilon, \quad \Delta^2 = \frac{1}{N} \sum_{0.3 < x < 0.8} [\varepsilon - m]^2 \quad (2)$$

where  $\varepsilon=[(T-T_{exp})/T_{exp}]$  and  $N=30$ . We observe (Table I) that the mixed 98 model gives the lowest values of the deviations averaged over the simulated H-mode dataset. We have also computed the deviation  $\Delta R_W$  defined in terms of the thermal energy [6], including in our simulated dataset 16 L-mode discharges from the ITER database. We find for the mixed 98 model the value of 0.14, which must be compared to a deviation of 0.15 for the best performing model tested so far [6].

TABLE I

MODEL	Mixed	Mixed 98	New Mixed
$\langle m_e \rangle$	0.06	0.015	0.09
$\langle \Delta_e \rangle$	0.07	0.06	0.10
$\langle m_j \rangle$	0.00	0.00	0.01
$\langle \Delta_j \rangle$	0.07	0.07	0.08



Figs.1-2 : Experimental electron temperature profile (solid line) compared to the profiles predicted by the mixed (dash), mixed 98 (dot-dash) and new mixed (dots) models.

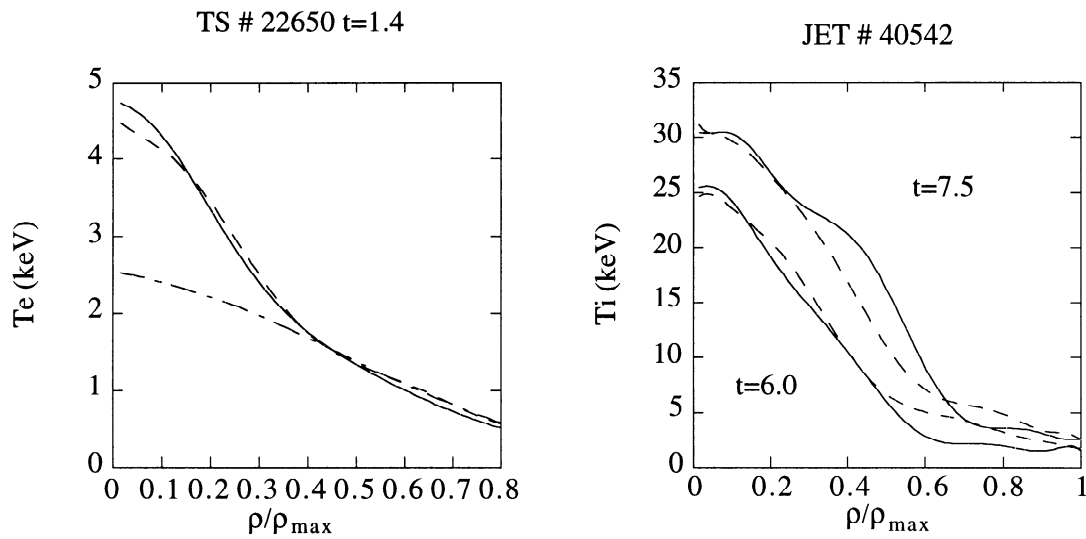
### 3. SIMULATIONS OF OPTIMIZED SHEAR DISCHARGES

The mixed 98 model can also describe the central ion and electron temperature rise typical of OS discharges if the Bohm term is reduced at low or negative magnetic shear or at high velocity shear rotation. The effect of shear in plasma rotation can be related to the ion pressure gradient through the electric field [7], and in this work we shall model this effect using a simplified expression [8]:

$$\chi_{B;e-i} \Rightarrow \chi_{B;e-i} \cdot \Theta \left( s + \frac{\nabla p_i}{\nabla p_{i-cr}} \right) \quad (3)$$

where  $\nabla p_{i-cr} = 100$  (keV/m<sup>4</sup>) and  $\Theta$  is the step function. We find that this expression describes well the position of the transport barrier in TS discharges with improved electron transport due to LH heating and current drive. As an example we consider the He discharge # 22650 with

$I_p=1$  MA,  $B_t=3.8$  T,  $P_{hyb}=1.6$  MW,  $a=0.77$  m,  $R=2.32$  m,  $\langle n_e \rangle = 2.3 \cdot 10^{19}$  m $^{-3}$ , characterized by improved central confinement during a quasi-stationary state ( Fig.(3) ).



Left: Fig.3: Experimental electron temperature profile (solid line) compared to the profiles predicted by the mixed 98 model with (dash) and without (dash-dot) shear function. Right: Fig.4: Experimental ion temperature profile (solid line) compared to the profiles predicted by the mixed 98 model (dash) for the L-mode (lower curves) and H-mode (upper curves) phase.

In the simulation of this discharge we have used data from the hard X-ray diagnostic for the shape of the power deposition profiles, considering the contribution of all energy channels [9]. While in the simulated TS shot the shear term dominates in eq. (3) and is the only responsible for improved confinement, the ion pressure gradient is more important than shear in controlling the movement of the ITB in OS JET discharges with NBI heating. Discharge # 40542 (with  $B_t \approx 3.4$  T,  $I_p \approx 3$  MA,  $P_{NBI} \approx 18$  MW) is well reproduced by our model in its L-mode and ELMy H-mode phases (Fig.(4)). The level of residual ion heat transport inside the barrier is mainly determined by the gyro-Bohm term

- [1] Erba M., et al., Plasma Physics and Controlled Fusion, Vol. **39** (1997) p. 261.
- [2] The JET TEAM, et al., IAEA, Montreal, Canada, 1996, IAEA-CN-64/AP1-2.
- [3] Connor J.W., et al., IAEA, Montreal, Canada, 1996, IAEA-CN-64/FP-21.
- [4] The JET Team, Plasma Physics and Controlled Fusion, **39** (1997) B353.
- [5] Pereverzev G.V., et al., IPP 5/42, August 1991.
- [6] Cordey J.G., Plasma Phys. and Contr. Fus. **39** (1997) B115.
- [7] Waltz R.E., et al., Phys. Plasmas **4** (1997) 2482.
- [8] Parail V.V., et al., JET-P(97)38.
- [9] Joffrin E., et al., this conference.